



Design and simulation Sandwich Composite Fairing Shells Using FEM Analyzing

Mahdi Jafari¹, Amir Kaveh^{2,*}, Amirreza Ardebili³, Omid Moini Jazani⁴

¹ *Department of Aerospace engineering, Malek Ashtar University of Technology, Tehran, Iran.*

² *Polymer Engineering Department, Amirkabir University of Technology, Tehran, Iran.*

³ *Composite Materials Department, Materials & Manufacturing Technology Faculty, Malek Ashtar University of Technology, Tehran, Iran.*

⁴ *Department of Chemical Engineering, Faculty of Engineering, University of Isfahan, Isfahan, Iran*

Abstract

In order to investigate and improve the destructive effects of maneuvers that the flying body has during a flight in space, it is necessary to know the forces acting on the flying body. In this paper, an analysis of the composite sandwich structure of a launch vehicle fairing is considered. This study explores carbon-fiber-reinforced skins with different cores used to deploy satellites and can be used as a space habitat. In order to calculate the effective forces on sandwich skins, finite element method (FEM) was used to determine three-dimensional stress and strain. Three types of structural models with honeycomb and solid core under dynamic loads were compared and evaluated. Models were compared in three category of stress distribution, strain and weight. The honeycomb core pattern helps reduce the structure's weight up to half of the structure compared to a solid core. The effect of mesh size sensitivity applied on simulations. The results showed that the amount of stress and strain were the same in all models and only differed in dispersion. However, the composite sandwich structure with aluminum core showed more strength against the applied forces.

Keywords: Honeycomb sandwich structures, Fairing, Satellite, Aerodynamic flight load, FEM Mesh Sensitivity.

1. Introduction

Satellites are subjected to many functional and structural tests from design to launch. Vibration, acoustic, and shock tests are the mechanical tests that satellites shall undergo before launch campaigns. The most important of these tests are the sine vibration tests. Verification and improvement of the structural design are directly related to the correlation between test results and calculations. Due to the increasing competition in the space industry today, it has become even more crucial to design the lightest and most effective satellite structure. A light satellite that achieves the requirements of the launcher means having a more beneficial transfer orbit and more payload. Besides, since the satellite launch cost is significantly reduced, the satellite service life in orbit increases [1]. To ensure

* Corresponding author. *E-mail address:* p90132910@aut.ac.ir

reliability during high-speed testing of aircraft products, preliminary design estimates of the strength and stability of structural units are required, taking into account the influence of various factors when the maximum speed of the test object is reached. The practical implementation of ground track tests of aircraft objects is preceded by mathematical modelling and the development of an algorithm for the numerical solution of a problem that simulates test conditions. The practical implementation of ground track tests of aircraft objects is preceded by mathematical modelling and the development of an algorithm for the numerical solution of a problem that simulates test conditions. The aerodynamic loading of the structure of the mobile track installation is considered using the methods of mathematical modelling and the development of an algorithm for the numerical solution of the problem of bending the elastic line of a cantilever tubular shell [2]. Satellites are subjected to many functional and structural tests from design to launch. Sine vibration, acoustic and shock tests are mechanical tests that satellites must apply out before launch. The most important of these tests is the vibration dynamic test. verification and improvement of structural design is related to the correlation between experimental and numerical results. Due to the incrementation in the space industry, the light satellite structure design has become vital. By reducing the weight, the cost of launching the satellite is significantly reduced and the service life of the satellite in orbit is increased [1]. To ensure reliability in high-speed testing of aircraft products, introductory design assessments of the strength and stability of structure are required, taking into account the influence of various factors when reaching the maximum velocity of the test body. Experimental test applied on a aircraft bodies by numerical modeling and development of an algorithm for numerical solution of a problem that simulates the test conditions [2].

Recently, many researchers have been investigated reliability-based analysis for payload fairing separation. Merrem et al. [3] covered in a paper, the aerodynamic vehicle body through the Mach number ranges from 5.0 to 0.8 by CFD simulations. The vehicle is equipped with multiple aerodynamic surfaces for navigating and lift forces. Mehta [4] presented an inverse analysis to estimate angle of attack, during the process of raising a satellite launch vehicle. Results computed numerically by solving three-dimensional (3D), time dependent equations over payload shell of a satellite launch vehicle. A controlled random search method is used to predict pitch, deflection and total angle of attack of vehicle. Transient differential pressure history in flight was measured from Mach numbers range of 0.5 to 3.0. Makhija et al. [5] considered a slender shell with spherical nose followed by the conical, cylindrical partitions. Simulations are applied at a Mach number of 0.95 with angle of attack of 0° , 2° , and 4° . ANSYS Fluent software was used for simulations. Density-based algorithm is used to obtain the steady state solutions with explicit time stepping. They are observed that as angle of attack increases, the normal shockwave moves towards nose, and the drag coefficient and pitching moment coefficients are found to increase. Ozair and Qureshi [6] presented in a paper transient CFD simulation of flow over a nose cone configuration. It was performed for a Mach number of 0.83. The objectives of their work were to compute the unsteady surface pressure variation and sound pressure levels. ANSYS Fluent software has been used in their study to perform two-dimensional (2D) Large Eddy Simulation (LES). Vitagliano et al. [7] described the experimental and numerical simulation of the Vega C space launcher in the range of Mach 0.5 and 3.5 behavior through the atmospheric flight volume. A large test matrix was considered with and without protrusions in the wind tunnel conditions. In the Hao et al. [8] proposed method, the augmented step size adjustment (ASSA) was employed. To further improve the efficiency, an adaptive substituted model was constructed to replace the time-consuming finite element analysis (FEA). Two mathematical criterions are used to validate the performance of the proposed method. Their payload fairing model demonstrated that the proposed framework is able to assess the reliability of fairing separation in an efficient and accurate manner. Vincenzino et al. [9] in a paper focused on the design solutions for CALLISTO's fairing. The concept of deployable aerodynamic surfaces was especially highlighted as the deployment causes a significant deflection of the vehicle's outsides. The module ANSYS Composite PrePost (ACP) was used to model the CFRP structure with accurate quantification of layered composite structures including material properties, assembly and orientation data of the layers. In a case study, Morovat et al. [10] proposed a fairing model of a launch vehicle (LV) using sandwich structures. Based on the theoretical sight, this concept caused a significant reduction in mass of fairing structure. Although sandwich structures application in the fairing of LV caused slight amount reduced 780kg of LV. The buckling of the conical composite sandwich shell was analyzed with the finite element method. Their results demonstrated that the discrepancies were negligible, reaching to 5% in the worst case. Cui et al. [11] improved dynamic simulation model of the satellite separation system considering the flexibility of interface rings. The impact evaluations of different parameters were carried out, respectively, by performing the sensitivity analysis on dynamic-envelope of clamp band and satellite separation shock responses. It was revealed from their study that the parameter which has the most prominent effect on the dynamic-envelope of clamp band was the stiffness of lateral spring. While for the axial and radial separation shock responses, the preload of clamp band and the density of V-segments are respectively the most influential parameters. Groves [12] developed a computational fluid dynamics

model and performed uncertainty analysis to confirm the spacecraft's airflow velocity requirements. Roshanian and Ebrahimi [13] used the Latin Hypercube sampling method (LHS) to calculate the reliability of the launch vehicle, and through sequential quadratic programming (SQP), reliability-based optimization was performed. Zhu et al. [14] investigated failure criteria of the separation system and the primary failure mode, and then they developed a series of connection reliability analysis models. However, the efficiency of the reliability assessment method for fair load separation needs to be further improved due to the unbearable computational load and complexity of fire load separation, in which large-scale uncertainty variables and several possible failure modes are involved.

Payload fairing separation is an essential process for various aerospace structures. Multiple source uncertainties in the fabrication and assembly processes must be considered further to ensure separation safety at the structural design stage. Reliability assessment is a powerful tool for dealing with multi-source uncertainties. However, the main challenge of numerical simulation of payload fairing separation is the high computational cost of structural analysis.

This study starts with a general description of the finite element model. In order to obtain accurate FEM, the structure of the sandwich composite fairing model interpreted. With the element size convergence, the valid element size of the FEM is chosen for dynamic analysis, and the model is generated. A practical payload fairing model is used to demonstrate the performance of the proposed framework. According to the result of global sensitivity analysis, those important variables that have a significant impact on the structural response are screened out.

2. Method of manufacturing

Due to the combined advantages of the core and sandwich structure, Honeycomb sandwich structures are extensively used in the aerospace and automotive industry to reduce the overall weight of vehicles, aircraft, and trains [15-18]. Examples of applications of Nomex honeycomb core sandwich structures in aircraft include floors, doors, wing wings, fuselage wing fenders, rudders, roof buckets, roof or sidewalls, engine bowls, spoilers, nozzles, and Other [17]. The Nomex honeycomb core is usually made of phenolic resin-impregnated aramid paper through an expansion process in which the core is composed of dual cell walls and single-cell walls. The dual cell wall is located along the Longitude direction (ribbon direction) of the Nomex nucleus, but a single cell wall is not. There are two layers of aramid paper in a dual cell wall that are bonded together by adhesive, but there is a layer of phenolic resin on the surfaces of each cell wall [19-21]. In reality, the honeycomb structure is neither geometrically perfect nor flawless. The specific manufacturing process is similar to some bond defects along the adhesive line in the two-cell wall.

A typical Nomex honeycomb core with 500 mm in length, 200 mm in width, and 21.6 mm in height is shown in Fig. 1. The core consists of hexagonal Nomex honeycombs with a cell size of 100 mm and a density of 48 kg/m³. The honeycombs were made from Nomex Type 412 aramid paper with a nominal thickness of 3 mm. The three directions of the honeycomb core are shown in Fig. 1.

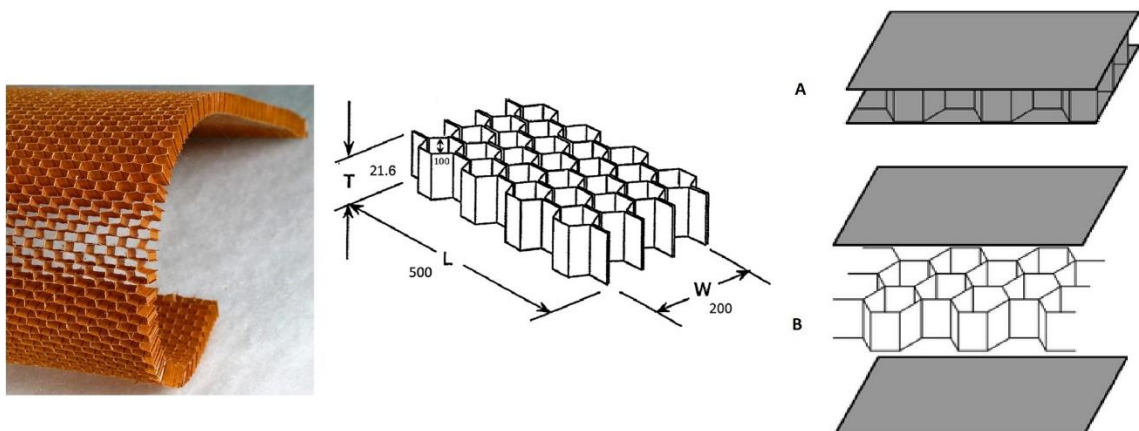


Fig. 1. Schematic and geometry of the Nomex honeycomb core (dimensions in mm).

Fig. 2 shows an embedded honeycomb core between two composite skins, where the large volume of air trapped inside the honeycomb core during layup could be a source for voids during cure. If all entrapped gasses are removed before curing, void sources will be reduced during curing, and the probability of honeycomb skin porosity will increase to the levels observed in monolithic laminates. The effectiveness of the vacuum retainer in air

evacuation depends on the pore space available for airflow.

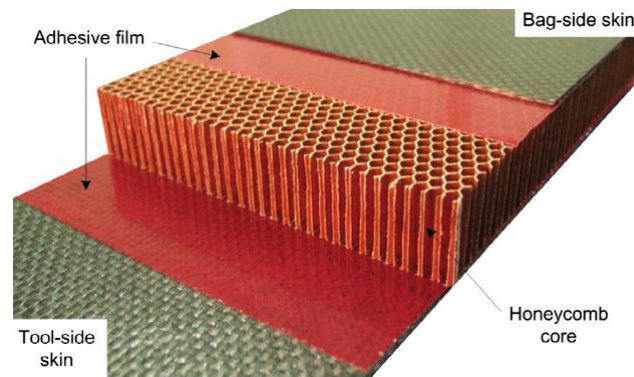


Fig. 2. Honeycomb sandwich panel components before cure [22].

In Fig. 3, a mechanism used to deformation shape the truss cores showed. The jig bars were stretched by pushing at their intersections (nodes) using hardened steel dowel pins. In order to soften the strain hardened bars and prevent dowel pin punch through at the nodes, two times intermediate annealing treatment (1100 °C for 15 minutes) was needed.

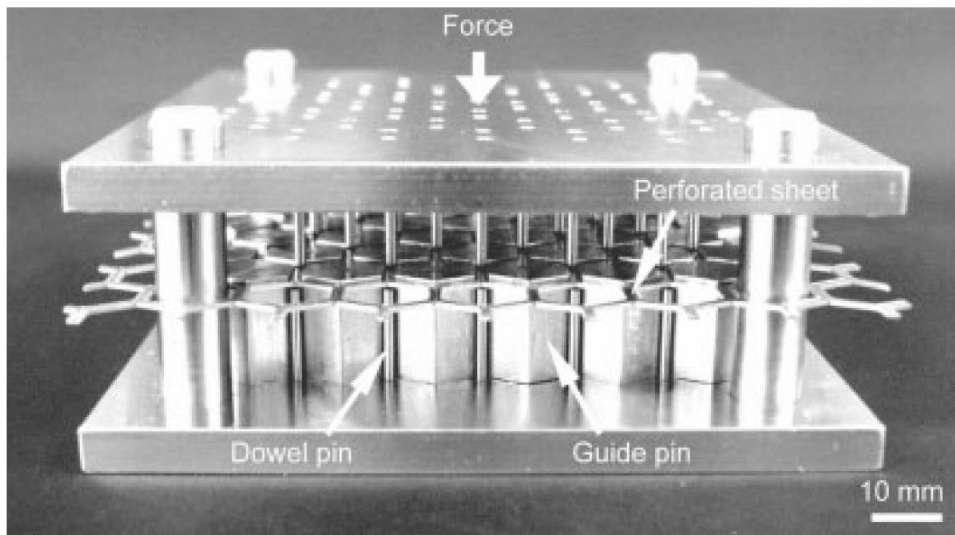


Fig. 3. Deformation shaping of the tetrahedral truss core [23].

3. Design and Simulation

A practical finite element model (FEM) of payload fairing is shown in Fig. 4. The diameter of the payload fairing is 1.5 m. The model is constructed and analyzed in ABAQUS 2020. As shown in Fig. 4, the fairing structure comprises a nose segment, cone segment, and barrel section. When the rocket reaches a certain height, the separation system will begin unlocking.

Finite element modeling and analysis was the primary tool used to design the fairing. Models were developed using available coupon samples and subscale test articles from various manufacturing alternatives and materials. The upper conic and barrel sections were designed assuming an oven-cured, vacuum bagged, sandwich composite, consisting of carbon-fiber/resin T300 face-sheets and honeycomb core made of Nomex and Al-5022. In the structural analysis, the elastic behavior of Nomex is defined using Liu's [24], and carbon-fiber/resin T300 is defined using Wang's [25] property research.

Table 1. Mechanical properties of the skin and the honeycomb core.

Properties	Value
Elastic Properties of T300 Carbon Fiber	
Longitudinal Young's Modulus E_1 (GPa)	230
Transvers Young's Modulus E_2 (GPa)	15
Longitudinal Shear Young's Modulus G_{12} (GPa)	15
Transvers Shear Young's Modulus G_{23} (GPa)	7
Major Poisson's Ratio ν_{12}	0.2
Transvers Poisson's Ratio ν_{23}	0.07
Mechanical Properties of Nomex core	
Density ρ (Kg/m ³)	1010
Elastic Modulus E (MPa)	3130
Poisson's Ratio μ	0.389
Mechanical Properties of Aluminum 5022 core	
Density ρ (Kg/m ³)	2680
Elastic Modulus E (MPa)	70300
Poisson's Ratio μ	0.33
Yield Strength σ_y (MPa)	193

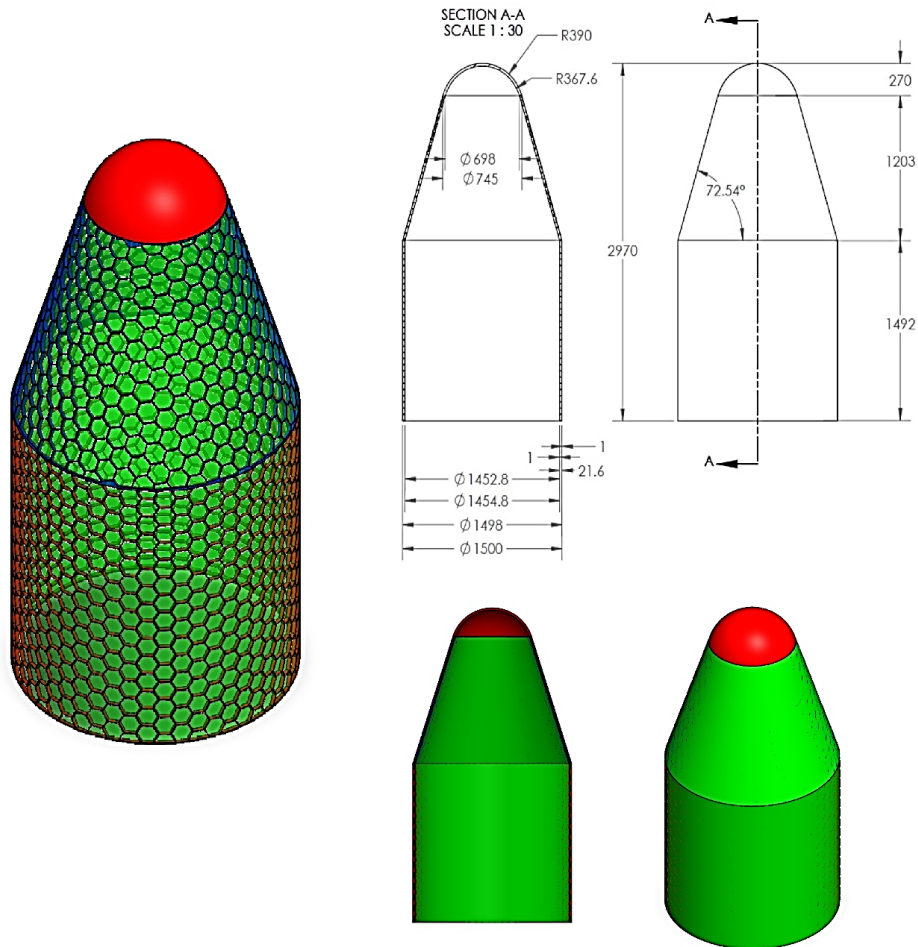


Fig. 4. Assembly model of the payload fairing (dimensions in millimeters).

The primary design loads included the maximum aerodynamic flight loads and the qualification loads. The

maximum aerodynamic high loads consisted of aerodynamic surface pressures, inertial loading, and a static pressure difference. Inertial loads were taken as 7g axially and 1g laterally. The internal pressure of 30 kPa was specified by the manufacturer. Fairing qualification loads were a combination of maximum bending and maximum dynamic pressure loads anticipated throughout the launch event. A summary of the load conditions' resultant forces and moments is given in Table 2. The load conditions were converted to equivalent strap loads, which correspond to the method of qualification testing. For model simulation and analysis, the strap loads were converted to equivalent pressure loads, then applied to the finite element model, as shown in the Fig. 5.

Table 2. Load conditions resultant forces and moment.

Component	Value
Axial	100 KN
Shear	63.2 KN
Bending Moment	48 KN.m

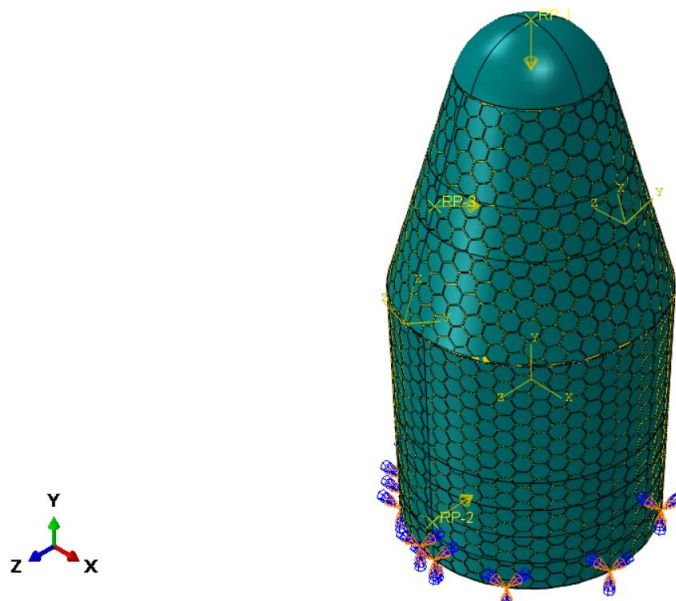


Fig. 5. The load conditions on the payload fairing.

The main idea of the proposed framework is to simplify the uncertainty model and employ a stable and efficient algorithm to perform reliability assessments. Dynamic Explicit finite element methods can be used to simulate such fairing analysis. The continuum shell 8-node quadrilateral elements SC8R and the 10-node modified quadratic tetrahedron elements C3D10M are used to model laminate parts and honeycomb parts in the explicit analysis step.

The mechanical interaction between laminate parts and honeycomb parts is modeled using three-dimensional general contact pairs, which in order to express mechanical contact properties, normal and tangential behavior frictionless was applied. The elements are located between adjacent surfaces of laminate parts, and honeycomb core parts can model the tie between two surfaces during the loading process. The rear bottom of the cylindrical parts was taken by the Encastre constraint ($U1=U2=U3=UR1=UR2=UR3=0$).

4. Model Results and Analysis

Based on the numerical simulation results, ABAQUS 2020 FEM explicit analysis has been performed to optimize the payload fairing components. The input loads are the maximum resulting contact forces that occur during fairing. This load case represents the most critical and realistic condition compared to an actual flight

scenario. The structural stress and deformation distribution with honeycomb aluminum core, Nomex core and solid core are shown in Figure 6 to 8, respectively. The highest concentration of stresses at the incorporation of vehicle parts was in the sample with aluminum honeycomb core and the lowest was in the sample with Nomex core. However, the magnitude of the stresses was lowest in the sample with the aluminum honeycomb core.

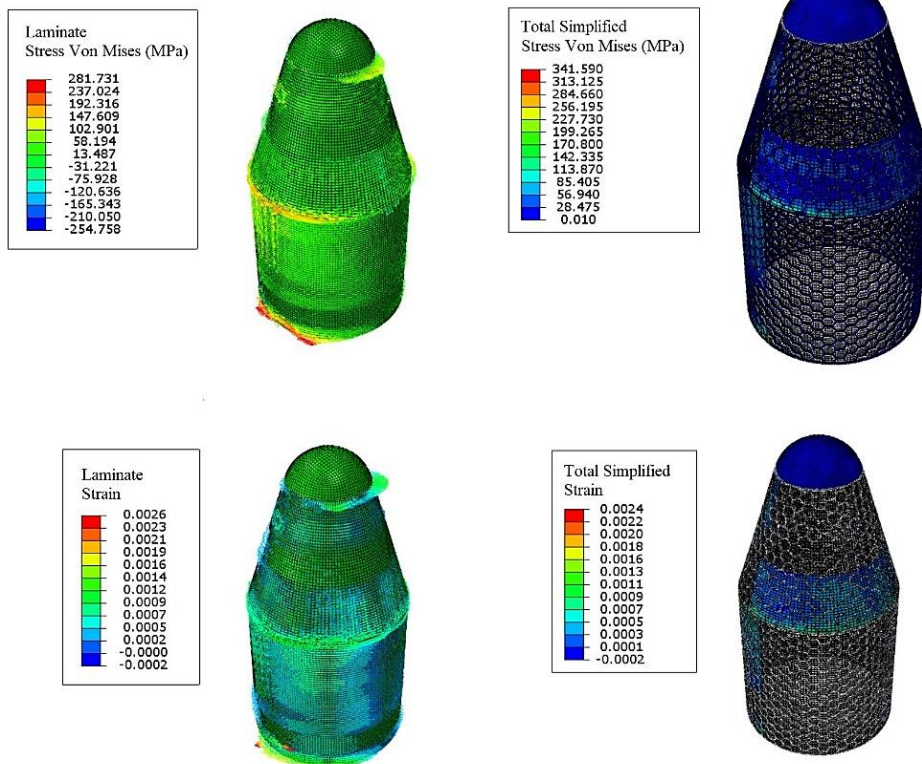


Fig. 6. Deformation and stress results with Al-5022 Honeycomb Parts 15mm and Laminate Parts 25mm mesh sizes.

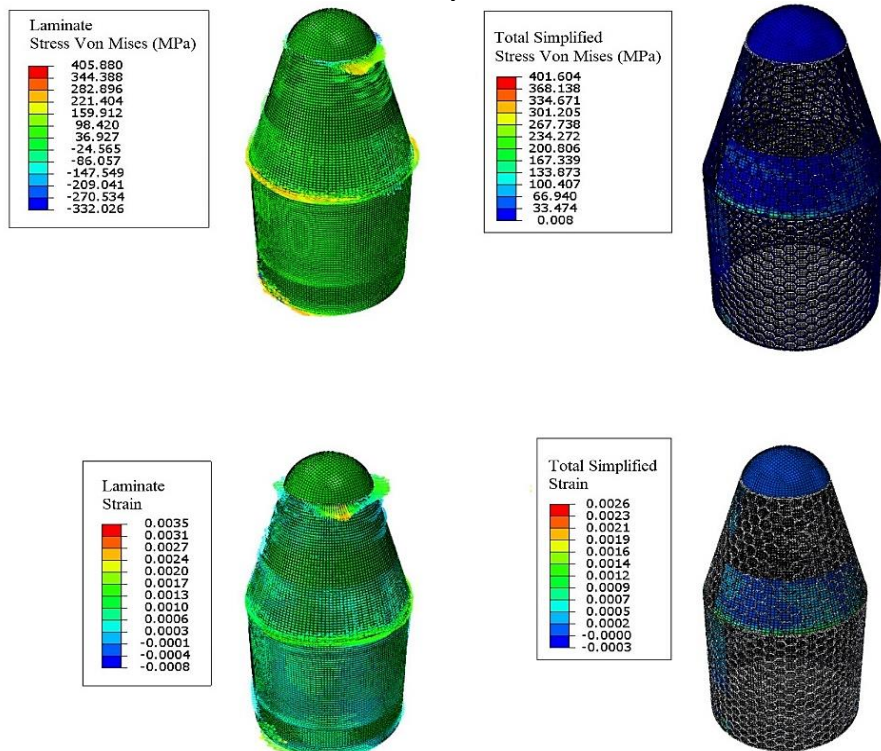


Fig. 7. Deformation and stress results with Nomex Honeycomb Parts 15mm and Laminate Parts 25mm mesh sizes.

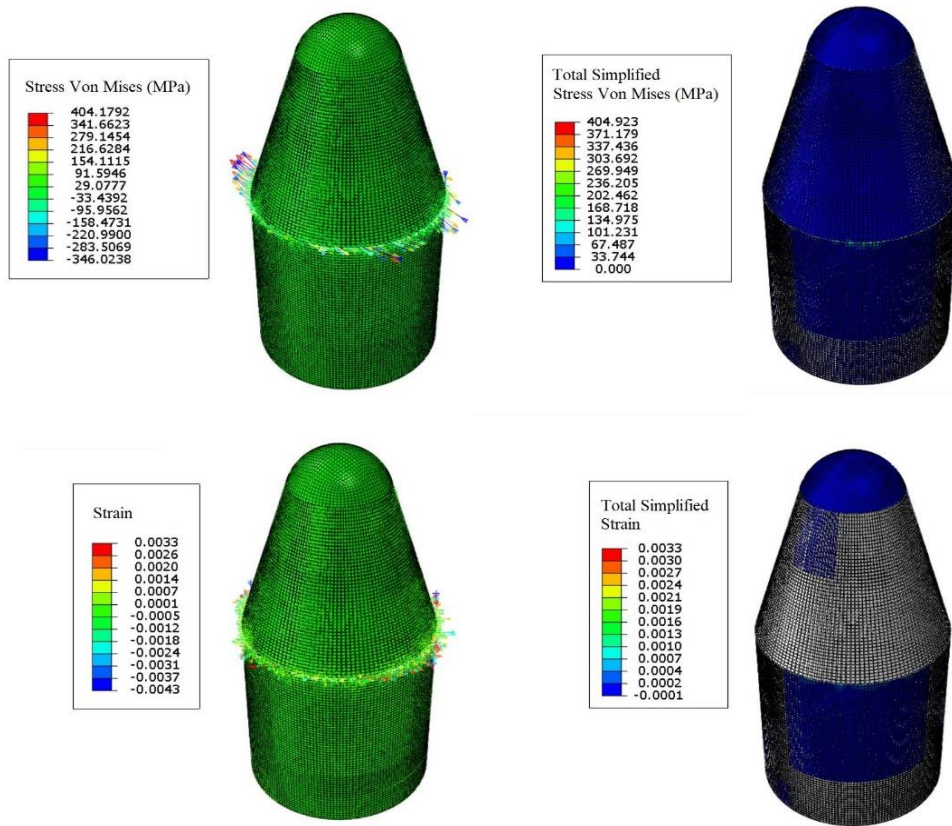


Fig. 8. Deformation and stress results with Al-5022 solid core with mesh size 25mm mesh size.

The aims of this section are to reduce the differences between results. Meshing size plays a vital role that if applied a more refined mesh at the vicinity of stress concentration region and a light bit coarser mesh at the far region compared to the mesh at the vicinity will get very quick and well convergence toward the exact solution. The effect of mesh size changes on results is shown in Tables 3-5. As can be seen in the results obtained from the sensitivity to the mesh, in the meshing range of 12.5-20 to 15-25, the results are adjacent, and the larger or smaller than this range, the results are coarser.

Table 3. Sensitivity of results accuracy with mesh modification for Aluminum core.

Part	Global Mesh Sizes					
	10	12.5	15	20	25	30
Honeycomb Parts	10	12.5	15	20	25	30
Laminate Parts	15	20	25	30	35	40
Maximum Stress (MPa)	574.6	385.7 7	341. 58	657 .03	408. 5	524.2 7
Maximum Strain	0.0029	0.002 4	0.00 24	0.0 022	0.00 21	0.002 1
Maximum Magnitude Displacement (mm)	4.0439	3.752 9	3.54 9	3.2 32	3.15 2	2.996

Table 4. Sensitivity of results accuracy with mesh modification for Nomex core.

Part	Global Mesh Sizes					
	10	12.5	15	20	25	30
Honeycomb Parts	10	12.5	15	20	25	30
Laminate Parts	15	20	25	30	35	40
Maximum Stress (MPa)	526.87	381.4	401. 603	263 .43	255 .19	239.6 2
Maximum Strain	0.0036	0.003 1	0.00 26	0.0 019	0.0 017	0.001 7
Maximum Magnitude Displacement (mm)	4.4971	4.121	3.87 8	3.7 01	3.5 68	3.472

Table 5. Sensitivity of results accuracy with mesh modification for a solid core.

Description	Global Mesh Sizes					
	15	20	25	30	35	40
Mesh sizes (mm)						
Maximum Stress (MPa)	587.65	394.4 3	404.2 7	388. 76	346. 25	325.7 5
Maximum Strain	0.0042	0.003 4	0.003 3	0.00 29	0.00 27	0.002 1
Maximum Magnitude Displacement (mm)	1.03	0.90	0.87	0.82	0.75	0.69

The aluminum honeycomb structure core reduces the weight of the structure by up to 1/3 of the solid aluminum structure core, and the Nomex honeycomb core reduces the weight of the structure up to 1/3 of the aluminum honeycomb core one. Table 6 shows the comparison weight of the structures.

Table 6. The weight of the whole model with a different core.

Description	Value
Payload fairing model with solid Al-5022 4mm thickness core	175 Kg
Payload fairing model with Al-5022 Honeycomb core	135 Kg
Payload fairing model with Nomex Honeycomb core	95 Kg

5. Conclusion

The bearing stresses of the fairing and the simulated aerodynamic pressure load is distributed in the ring shape. The maximum stress is close to the connection between the head and the cone section, the cone, and the cylindrical section. The smallest is at the top of the head and gradually increases along the axial direction, and the cylinder section stress is more equally distributed.

The displacement distribution of the fairing head has the largest amount, which gradually decreases along the axial direction and has a circular distribution. The displacement of the rear section of the cylindrical section gradually increases. The strain is also distributed in the ring shape, but the deformation strain of the head and the cylindrical section is relatively small, the strain in the middle area is relatively large, and the strain in the head area is the largest, so it is necessary to focus on the optimal design of cone and head section.

The composite sandwich structure with aluminum core showed more strength against the applied forces, but the composite sandwich structure with Nomex core also showed acceptable results, which the amount of stress and strain bearing of the sample with honeycomb aluminum core was up to 2 times higher than the sample with honeycomb Nomex core one.

The results converged in the mesh range of 12.5-15mm in Honeycomb parts and 20-25mm in laminate parts. Smaller or larger than this range of the mesh sizes fluctuated and was not correct. The amount of stress and strain applied was almost the same on all three models, but the stress and strain distribution differed. As in the case of solid aluminum core, almost the whole structure was equally distributed, and the highest distribution was related to the structure with Nomex core.

According to [26], Satellites can be categorized with respect to the mission objective, maximum mass and operational orbit. The second criterion, which is the mass of the spacecraft, with respect to the mass of the spacecraft, there are three types of spacecrafts. Large spacecraft are greater than 1000 kg and the mass of medium spacecraft is between 500 kg to 1000 kg with propellants. With a mass of less than 500 kg, spacecraft can be classified as small spacecraft [1]. The models that were analyzed classified into small spacecraft categories. Three types of design that were modeled and analyzed, the lightest with the Nomex core and the safest and optimized one was with the honeycomb aluminum core. Using the Nomex honeycomb structure can reduce the structure's weight to half of the solid aluminum core type.

References

- [1] A. Çekiç, *Improvement of finite element model by using sine vibration test results of a communication satellite*, Thesis, Middle East Technical University, 2021.
- [2] S. A. Astakhov, V. I. Biryukov, Buckling under the action of loading by aerodynamic and inertial forces during ground track tests of aviation equipment, *INCAS Bulletin*, Vol. 13, pp. 5-12, 2021.
- [3] C. Merrem, V. Wartemann, T. Eggers, Preliminary aerodynamic design of a reusable booster flight experiment, *CEAS Space Journal*, Vol. 12, No. 3, pp. 429-439, 2020.
- [4] R. Mehta, Estimation of Angle of Attack in Satellite Launch Vehicle Using Flush Air Data Sensing Systems at Mach 0.5 to 3.0, *Sch J Eng Tech*, Vol. 7, pp. 77-86, 2021.
- [5] J. Makhija, D. S. K. Reddy, Numerical simulation of flow field over slender bodies at transonic Mach number and low angle of attacks, in *Proceeding of*, IOP Publishing, pp. 042047.
- [6] M. Ozair, M. N. Qureshi, Numerical Prediction of Aeroacoustic Loads on a Hammerhead Nose Cone Configuration, in *Proceeding of*, IEEE, pp. 806-810.
- [7] P. Vitagliano, F. De Gregorio, P. Roncioni, F. Paglia, C. Milana, AERODYNAMIC CHARACTERISATION OF VEGA-C LAUNCHER.
- [8] P. Hao, Z. Li, S. Feng, W. Li, Y. Wang, B. Wang, A novel framework for reliability assessment of payload fairing separation considering multi-source uncertainties and multiple failure modes, *Thin-Walled Structures*, Vol. 160, pp. 107327, 2021.
- [9] S. G. Vincenzino, W. Rotärmel, I. Petkov, H. Elsässer, E. Dumont, L. Witte, S. Schröder, Reusable structures for callisto, in *Proceeding of*.
- [10] F. Morovat, A. Mozaffari, J. Roshanian, H. Zare, A novel aspect of composite sandwich fairing structure optimization of a two-stage launch vehicle (Safir) using multidisciplinary design optimization independent subspace approach, *Aerospace Science and Technology*, Vol. 84, pp. 865-879, 2019.
- [11] D. Cui, J. Zhao, S. Yan, X. Guo, J. Li, Analysis of parameter sensitivity on dynamics of satellite separation, *Acta Astronautica*, Vol. 114, pp. 22-33, 2015.
- [12] C. E. Groves, *Dissertation Defense Computational Fluid Dynamics Uncertainty Analysis for Payload Fairing Spacecraft Environmental Control Systems*, pp. 2014.
- [13] J. Roshanian, M. Ebrahimi, Latin hypercube sampling applied to reliability-based multidisciplinary design optimization of a launch vehicle, *Aerospace Science and Technology*, Vol. 28, No. 1, pp. 297-304, 2013.
- [14] X. Zhu, H. Li, T. Yu, B. Song, Research on reliability analysis for low-altitude and high-speed payload fairing separation, in *Proceeding of*, IEEE, pp. 90-94.
- [15] A. Gilioli, C. Sbarufatti, A. Manes, M. Giglio, Compression after impact test (CAI) on NOMEX™ honeycomb sandwich panels with thin aluminum skins, *Composites Part B: Engineering*, Vol. 67, pp. 313-325, 2014.
- [16] Y.-B. Park, J.-H. Kweon, J.-H. Choi, Failure characteristics of carbon/BMI-Nomex sandwich joints in various hygrothermal conditions, *Composites Part B: Engineering*, Vol. 60, pp. 213-221, 2014.
- [17] R. Roy, K. Nguyen, Y. Park, J. Kweon, J. Choi, Testing and modeling of Nomex™ honeycomb sandwich Panels with bolt insert, *Composites Part B: Engineering*, Vol. 56, pp. 762-769, 2014.
- [18] X. Xue, C. Zhang, W. Chen, M. Wu, J. Zhao, Study on the impact resistance of honeycomb sandwich structures under low-velocity/heavy mass, *Composite Structures*, Vol. 226, pp. 111223, 2019.
- [19] Z. Zhao, C. Liu, L. Sun, H. Luo, J. Wang, Y. Li, Experimental and numerical study on the constrained bending-induced collapse of hexagonal honeycomb, *Composite Structures*, Vol. 277, pp. 114604, 2021.
- [20] A. Karakoç, K. Santaoja, J. Freund, Simulation experiments on the effective in-plane compliance of the honeycomb materials, *Composite Structures*, Vol. 96, pp. 312-320, 2013.
- [21] R. Roy, S.-J. Park, J.-H. Kweon, J.-H. Choi, Characterization of Nomex honeycomb core constituent material mechanical properties, *Composite Structures*, Vol. 117, pp. 255-266, 2014.
- [22] J. Kratz, P. Hubert, Anisotropic air permeability in out-of-autoclave prepregs: Effect on honeycomb panel evacuation prior to cure, *Composites Part A: Applied Science and Manufacturing*, Vol. 49, pp. 179-191, 2013.
- [23] D. J. Sypeck, H. N. Wadley, Cellular metal truss core sandwich structures, *Advanced Engineering Materials*, Vol. 4, No. 10, pp. 759-764, 2002.
- [24] L. Liu, P. Meng, H. Wang, Z. Guan, The flatwise compressive properties of Nomex honeycomb core with debonding imperfections in the double cell wall, *Composites Part B: Engineering*, Vol. 76, pp. 122-132, 2015.
- [25] W. Wang, Y. Dai, C. Zhang, X. Gao, M. Zhao, Micromechanical modeling of fiber-reinforced composites with statistically equivalent random fiber distribution, *Materials*, Vol. 9, No. 8, pp. 624, 2016.

- [26] G. Di Mauro, M. Lawn, R. Bevilacqua, Survey on guidance navigation and control requirements for spacecraft formation-flying missions, *Journal of Guidance, Control, and Dynamics*, Vol. 41, No. 3, pp. 581-602, 2018.